

Can Feedback Solve the Too Big to Fail Problem?

Shea Garrison-Kimmel^{*}, Miguel Rocha, Michael Boylan-Kolchin[†],
James S. Bullock, Jaspreet Lally

Center for Cosmology, Department of Physics and Astronomy, University of California, Irvine, CA 92697, USA

16 January 2013

ABSTRACT

The observed central densities of Milky Way dwarf spheroidals (dSphs) are significantly lower than the densities of the largest ($V_{\max} \sim 35$ km/s) subhalos found in dissipationless simulations of Galaxy-size dark matter hosts. One proposed solution is that gas removal from feedback can lower core densities enough to match observations and that repeated bursts can aid in this process. We use high-resolution, idealized simulations to explore the effects of time-varying central potentials on the density distributions of dwarf dark matter halos, mimicking repeated bursts of baryonic feedback. We find that for the same mass of gas removed, cyclic blow-outs are *less effective* at lowering dark matter densities than a single large burst. In order to match the observed densities of $M_{\star} \sim 10^6 M_{\odot}$ dSphs, the energy equivalent of more than 40,000 supernovae must be delivered with 100% efficiency directly to the dark matter. This exceeds the number of supernovae that have ever exploded for typical initial mass functions. The mass-loading required is also significant. More than 500 times the total mass in stars today must be ejected from these galaxies, a mass that exceeds the baryonic allotment for the halos of concern. Based on these results, we conclude that it is unlikely that episodic supernova feedback can solve the “Too Big to Fail” problem for Milky Way subhalos.

Key words: dark matter – cosmology: theory – galaxies: haloes – Local Group

1 INTRODUCTION

The current paradigm for structure formation, cold dark matter with a cosmological constant (Λ CDM), has proven successful at reproducing the large scale universe (Hinshaw et al. 2012; Ho et al. 2012, and references therein); however, disparities exist between the theory and observations on small scales. For example, the rotation curves of dwarf and low surface brightness (LSB) galaxies appear to favor core-like density distributions rather than the cuspy distributions seen in dissipationless simulations (Flores & Primack 1994; Moore 1994; Kuzio de Naray et al. 2008; Trachternach et al. 2008; de Blok 2010; Kuzio de Naray & Kaufmann 2011). There has been much discussion in the literature regarding the ability of baryonic processes, i.e. feedback, to displace dark matter and resolve the problem (Navarro et al. 1996; Mashchenko et al. 2006; Pontzen & Governato 2012; Ogiya & Mori 2012; Teyssier et al. 2012) – such arguments seem reasonable given the stellar mass ($M_{\star} \sim 10^8 M_{\odot}$) of a typical LSB galaxy.

More troubling is that a similar problem appears to ex-

ist for even lower luminosity dwarf spheroidal (dSph) galaxies ($M_{\star} \sim 10^6 M_{\odot}$) in the Local Group (Boylan-Kolchin et al. 2011, 2012). This issue, nicknamed the “Too Big To Fail” (TBTf) problem, points out that the largest subhalos in high resolution collisionless simulations (Diemand et al. 2008; Springel et al. 2008) are too dense at their centers to host any of the dSphs around either the Milky Way or Andromeda (Tollerud et al., in preparation). The problem is summed up in Figure 1, in which a rotation curve typical of one of these “massive failures” is plotted along with observational data from Wolf et al. (2010) for all the bright dSphs around the Milky Way. If the largest subhalos do host the bright dwarfs, then the dark matter must be less dense in their centers than predicted in dissipationless CDM simulations, either because of baryonic processes (e.g. Brooks & Zolotov 2012; Arraki et al. 2012) or non-standard dark matter physics (e.g. Vogelsberger et al. 2012; Rocha et al. 2012).

While feedback appears a plausible solution to the cusp/core problem in brighter dwarf galaxies and LSBs, dSph galaxies are much more dark matter dominated, with observed mass-to-light ratios within the stellar radius in excess of 100 in some cases (e.g. Walker 2012). Moreover, according to the theoretical extrapolation of abundance

^{*} sgarriso@uci.edu

[†] Center for Galaxy Evolution fellow

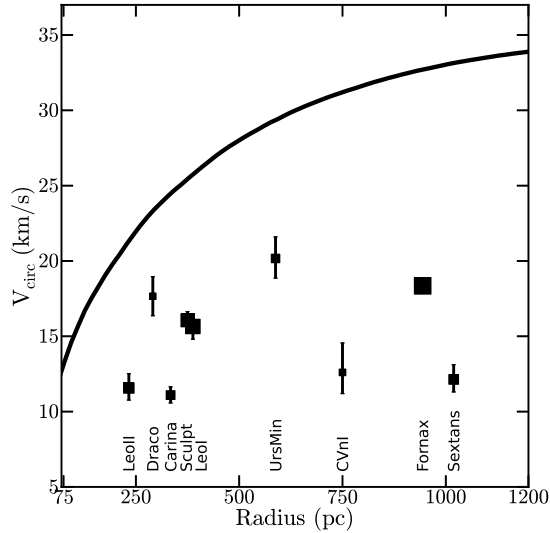


Figure 1. The simulated circular velocity profile as a function of subhalo radius along with observed circular velocities. The solid line shows the circular velocity profile of our idealized halo in the initial conditions, which is representative of the largest subhalos found in dark-matter-only simulations of Milky Way-size halos, a Too Big to Fail subhalo. The data, taken from Wolf et al. (2010), are observationally derived values for all the bright dSphs; the size of the points is proportional to the luminosity of that satellite. The Milky Way’s satellites have significantly less mass near their center than the halos in which abundance matching predicts they form.

matching, we expect the stellar mass to drop by ~ 2.5 dex for a difference of only one decade in halo mass at these mass scales (Behroozi et al. 2012). The expectation is that the dark matter’s gravitational potential should overwhelm that of the baryons, even at the centers of halos. Finally, the fact that these systems are so deficient in stars means that the total energy available to alter the gravitational potential is minimal. Recently, Peñarrubia et al. (2012) highlighted the tension associated with the need to suppress star formation in small dark matter halos while simultaneously lowering their central densities. In this paper we use focused simulations to explore whether blow-out feedback of any kind can realistically solve the TBTF problem given the minimal stellar content of the Milky Way dSphs.

Some groups (e.g. Governato et al. 2012; Zolotov et al. 2012; Teyssier et al. 2012) have successfully reproduced the low densities of LSBs and larger dwarfs by invoking supernovae feedback in cosmological zoom-in simulations of galaxies. Dwarf spheroidals present a much more difficult problem numerically because of their small physical size ~ 300 pc and associated stellar mass $\sim 10^7 M_\odot$ (Strigari et al. 2008). Indeed, the central regions of dSph halos remain extremely difficult to resolve in collisionless zoom simulations (Boylan-Kolchin et al. 2012), let alone hydrodynamical simulations. Poor resolution can give rise to two-body relaxation errors that tend to flatten the inner density profile; this undesired effect propagates radially outwards in the cumulative velocity profile. Moreover, if the dark matter potential is shallower due to the lack of adequate resolution, gas outflows

and tidal effects may over-predict the removal of mass. These issues motivate our use of controlled, idealized simulations to achieve the required force (~ 10 pc) and mass resolution ($\sim 1000 M_\odot$).

In what follows, we examine the effects of feedback on isolated dark matter halos with peak circular velocities of ~ 35 km/s, the mass range associated with TBTF halos (Boylan-Kolchin et al. 2012). We mimic baryonic feedback using an externally tunable gravitational potential. This allows us to test the amount of gas that must be removed from the center of the halo in order to bring the circular velocity into agreement with observations, as well as the energy required to do so. Our implementation also allows us to test whether cyclic blowouts are effective at removing dark matter, as discussed by Pontzen & Governato (2012), and their relative efficiency compared to a single blowout of the same total mass.

The layout of this work is as follows: in §2, we describe our methods for producing the initial conditions and for emulating star formation cycles, as well as present a resolution test; in §3, we study the dark matter distribution as a function of gas blown out and investigate the energetic requirements; finally, in §4, we discuss the results, focusing specifically on the implications for the Too Big to Fail problem.

2 SIMULATIONS

2.1 Initial Conditions

Cosmological abundance matching models predict that galaxies with $L_V \sim 10^5 L_\odot$ form in dark matter halos with $V_{\max} \sim 35$ km/s (Guo et al. 2010). Moreover, the five largest subhalos found in simulations of Milky Way-size halos typically have $V_{\max} > 35$ km/s (Boylan-Kolchin et al. 2012). This pinpoints halos with $V_{\max} \sim 35$ km/s as a characteristic size of concern. Such a halo (with the circular velocity curve peaking at a radius of 2.2 kpc, as expected for subhalos) is shown in Figure 1; the data are circular velocity curve measurements at the half light radii $r_{1/2}$ of each of the nine brightest Milky Way dSphs (Wolf et al. 2010). Six of these nine have luminosities $L_V < 10^6 L_\odot$. The data points are sized in proportion to their luminosities, which range from $L_V = 2.2 \times 10^5 L_\odot$ (Draco) to $1.7 \times 10^7 L_\odot$ (Fornax). Their associated densities are clearly low compared to both the naive expectations of abundance matching and the expected densities of the most massive Milky Way subhalos.

With this as motivation, we initialize a dark matter halo with $V_{\max} = 35$ km/s at 2.2 kpc using a Hernquist 1990 sphere, which follows the roughly-expected $\rho \propto r^{-1}$ dependence at small radius. We do this by self-consistently sampling the phase space distribution function of the model (see also Kazantzidis et al. 2004; Bullock & Johnston 2005; Zemp et al. 2008). As long as the resolution is appropriate, generating initial conditions in this manner can produce systems that stay in equilibrium for over a Hubble time (Kazantzidis et al. 2004). We have developed a code that applies this technique to generate initial conditions for a variety of density profiles assuming isotropic velocity dispersions. Our code, named *spherIC*, is publicly available¹ and can also generate systems with an embedded stellar component that follows

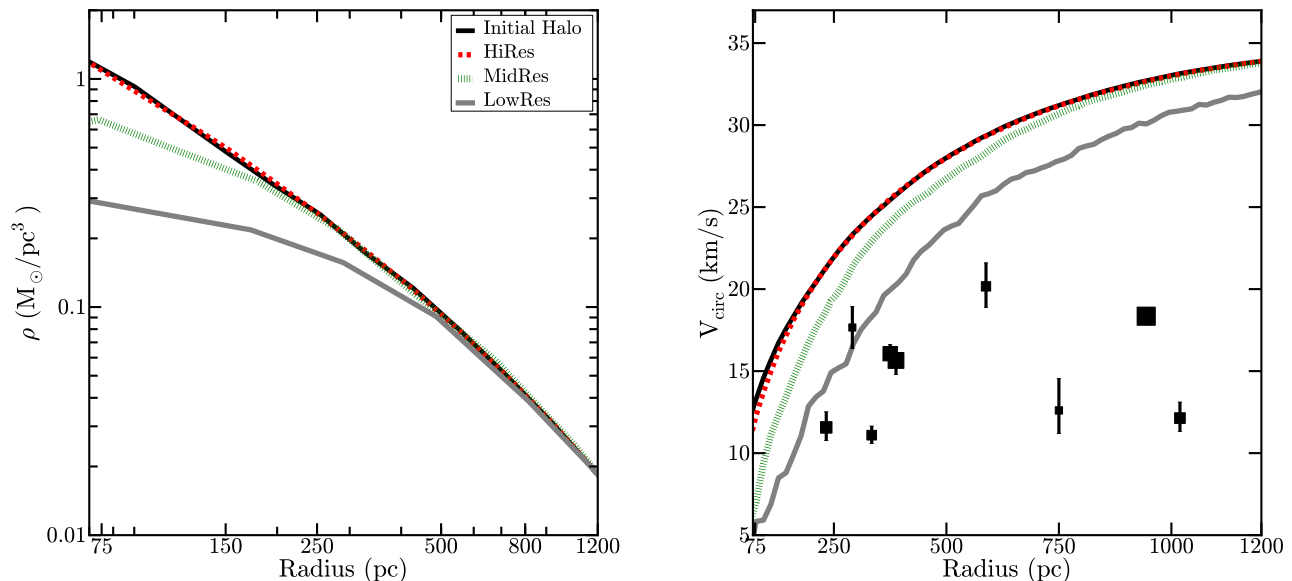


Figure 2. Resolution test. Plotted are the density (left) and circular velocity (right) profiles for the isolated halo initially (solid black) and after running with no external potential for 5 Gyr with three different mass and force resolutions as labeled in the caption and in Table 1. Note that the highest resolution Milky Way cosmological simulations that have been run and can test feedback effects on dSph satellites have resolutions comparable to our LowRes runs (Guedes et al. 2011; Brooks & Zolotov 2012). Although the density converges in the LowRes run at ~ 500 pc, the circular velocity does not converge until beyond 1 kpc. Since only the HiRes run does not suffer from numerical effects in the regions of interest, we use this resolution exclusively for the experiments presented in the rest of this paper.

its own density distribution, chosen from a set of profiles typical for stellar systems.

In order to ensure that our results are stable to numerical effects, we simulate our initial halo in isolation at increasing force ($\epsilon = 10, 70, 120$ pc) and mass ($m_p = 760, 24000, 150000 M_\odot$) resolution as detailed in Table 1. Figure 2 shows the resultant density and circular velocity profiles after 5 Gyr for each of these runs. We note that the highest resolution hydrodynamic simulations to date that have been performed to test baryonic feedback effects on dwarf satellites in Milky Way-mass halos have been run with force softenings comparable to our *lowest* resolution test (Guedes et al. 2011; Zolotov et al. 2012; Pontzen & Governato 2012). We see that the circular velocity curves for runs at this resolution are under-resolved at all relevant radii. Though numerical effects set in at $\sim 4\epsilon$ in density, the cumulative circular velocity remains divergent to much larger radii. To ensure that the circular velocity has converged at radii comparable to observed values of $r_{1/2}$, which range as low as ~ 250 pc, the remainder of our work relies on simulations with $760 M_\odot$ particles and 10 pc force resolution, equivalent to the HiRes runs shown in Figure 2.

2.2 Modeling Gas Blowouts

We model a star formation cycle (i.e. gas accretion onto a central galaxy and the subsequent ejection of that gas) by varying the properties of a spherically-symmetric gravitational potential placed at the center of the halo. Specifically,

Simulation	$m_p (M_\odot)$	ϵ (pc)	N_p
HiRes	7.6×10^2	10	3,000,000
MidRes	2.4×10^4	70	96,891
LowRes	1.5×10^5	120	30,000

Table 1. Parameters of the runs used in the resolution test (Figure 2) where ϵ is the Plummer-equivalent softening length. The remainder of the simulations we discuss in this paper use the HiRes parameters.

we added an externally tunable Hernquist potential to the N-body code Gadget2 (Springel 2005) such that each particle has an additional acceleration given by

$$\vec{a} = \frac{-GM_{\text{gal}}(t)}{[r + b(t)]^2} \frac{\vec{r}}{r}, \quad (1)$$

where $M_{\text{gal}}(t)$ is the total mass in the potential at time t and $b(t)$ is related to the half-mass radius of the potential, $r_{1/2}$, by $r_{1/2} = b/(\sqrt{2} - 1)$. To prevent the acceleration of a particle from becoming unphysically large when $r \rightarrow 0$, we “soften” the potential by setting $\vec{r}/r \rightarrow \vec{r}/\epsilon$ when $r < \epsilon$, the Plummer-equivalent softening length.

Our implementation allows us to specify the properties of the potential (M_{gal} and $r_{1/2}$) at any time. Our fiducial runs fix $r_{1/2}$ and vary M_{gal} . Most of our runs force $r_{1/2} = 500$ pc, which is a typical half-light radius among the bright Milky Way dSphs. We vary M_{gal} over a series of cycles, with a fiducial period of 500 Myr (see Figure 3). Specifically, M_{gal} grows linearly from zero over 200 Myr to its maximum

¹ <https://bitbucket.org/migroch/spheric>

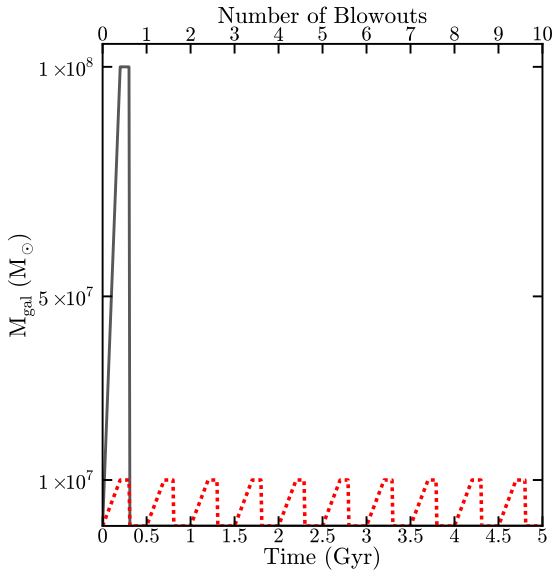


Figure 3. A representative example of our blowout scheme. Plotted is the mass in the central potential as a function of time for two of our runs that blow out the same total amount of gas. In grey is the mass as a function of time for a single blowout with $M_{\text{max}} = 10^8 M_{\odot}$; the red dotted line shows the same for repeated blowouts with $M_{\text{max}} = 10^7 M_{\odot}$. A single cycle takes 500 Myr. These two cases result in the same cumulative total of mass displaced, but as shown in Figure 4, the single large burst affects the dark matter density to a larger extent.

mass, M_{max} , then remains constant for 100 Myr to allow the halo to come to equilibrium. We then mimic a blow-out by forcing M_{gal} to instantaneously return to zero, where it remains for 200 Myr before beginning the next cycle. We have tested a number of other models for blowouts, including those with different periods, models without a relaxation time, sinusoidal modulations, models with M_{gal} constant and $r_{1/2}$ varying. The model we show here produces the maximal effect on the rotation curve, though the qualitative results are very similar in most cases. The only exception is the sinusoidal model, which is symmetric and effectively produces no change in the density distribution.

In what follows we present results for models with $M_{\text{max}} = 10^6 M_{\odot}$, $10^7 M_{\odot}$, $10^8 M_{\odot}$, and $10^9 M_{\odot}$. For each of these we vary M_{gal} from zero to M_{max} and back to zero ten times over a total of 5 Gyr. We output snapshots after every blowout, so that we can investigate the effect of any number of star formation cycles on the associated dark matter profile. For example, the grey line in Figure 3 illustrates the galaxy mass as a function of time over one cycle of $10^8 M_{\odot}$ while the red line shows ten cycles of $10^7 M_{\odot}$ each – in both of these runs, a total of $10^8 M_{\odot}$ is blown out from the halo. We also test how strongly the results depend on the scale radius by presenting new runs with $r_{1/2} = 100$ pc and $M_{\text{max}} = 10^7 M_{\odot}$ and $10^8 M_{\odot}$.

3 RESULTS

Figure 4 shows changes in the density and circular velocity profiles of our initial halo after undergoing blowout(s) of

various masses. We directly compare ten blowouts of $10^7 M_{\odot}$ ($10^8 M_{\odot}$) to one blowout of $10^8 M_{\odot}$ ($10^9 M_{\odot}$), and find that for both values of M_{max} , a single blowout (grey line in Figure 3) removes more mass from the center of the halo than repeated blowouts that amount to the same total mass removed (red line in Figure 3). While we do see some evidence that cyclic, lower mass blowouts remove mass preferentially from the inner regions compared to a more massive blowout, being more effective at forming a “core,” the density distribution never becomes perfectly flat in the center – some degree of cuspsiness always remains.

Figure 4 illustrates that in order to bring our fiducial TBTF halo (solid black) into agreement with the density of a typical dSph, a total of $\sim 10^9 M_{\odot}$ of material must be removed from the halo in either one massive blowout (dashed green, the biggest effect) or in a few repeated smaller blowouts (solid blue) totaling this amount. A first-order check suggests that this is at the edge of plausibility from the standpoint of baryon fraction. This mass exceeds the entire baryonic allotment for a field halo of $M_{\text{vir}} \simeq 5 \times 10^9 M_{\odot}$, which is the mass associated with an $M_{\star} \simeq 10^6 M_{\odot}$ galaxy according to the extrapolated abundance matching of Behroozi et al. (2012) and also the virial mass associated with a typical TBTF halo at the time of infall (Boylan-Kolchin et al. 2012).

A more general presentation of our results is given in Figure 5. Each panel shows the dark matter remaining within 500 pc after multiple blowout runs. On the left, we present the mass of dark matter remaining as a function of total mass ejected and on the right we show the same quantity as a function of the total energy added to the dark matter (see below). For reference, the horizontal dotted line shows the initial dark matter mass within 500 pc and the shaded horizontal bands show estimates of the dark matter mass within 500 pc for three representative dwarfs, as determined in Boylan-Kolchin et al. (2012).

In the left panel of Figure 5, the different symbol types correspond to different values of the mass blown out per cycle, spanning $10^6 M_{\odot}$ to $10^9 M_{\odot}$ as indicated in the figure. Multiple points with the same symbol type correspond to repeated blowouts of the same mass. The points here are from runs with $r_{1/2} = 500$ pc. As discussed above, a single massive blowout removes more mass from the center of the halo than the cumulative effect of 10 smaller blowouts that result in the same total mass expelled. For reference, the upper axis shows the implied mass loading factor, normalized for a dSph with $M_{\star} = 10^6 M_{\odot}$. We see that a minimum of $7 \times 10^8 M_{\odot}$ of material must be removed in order to reach the observed density of the densest dwarfs shown, Ursa Minor (cyan band). This would imply a cumulative mass loading factor of ~ 1000 if we assume a stellar mass-to-light ratio of $M_{\star}/L_V = 2$ for this system.

The mass of Fornax is represented by the grey band. Though the density of Fornax is significantly lower than that of Ursa Minor, it may be the easiest dwarf to explain because its reservoir of stars is much greater ($M_{\star} \simeq 4 \times 10^7$). We see that a cumulative expulsion of $\sim 10^9 M_{\odot}$ can in principle match the central density of Fornax, which would require a more modest – though still large – mass-loading of ~ 25 . However, this is only one system and it does not explain the unexpectedly low densities of the other, less luminous dwarfs.

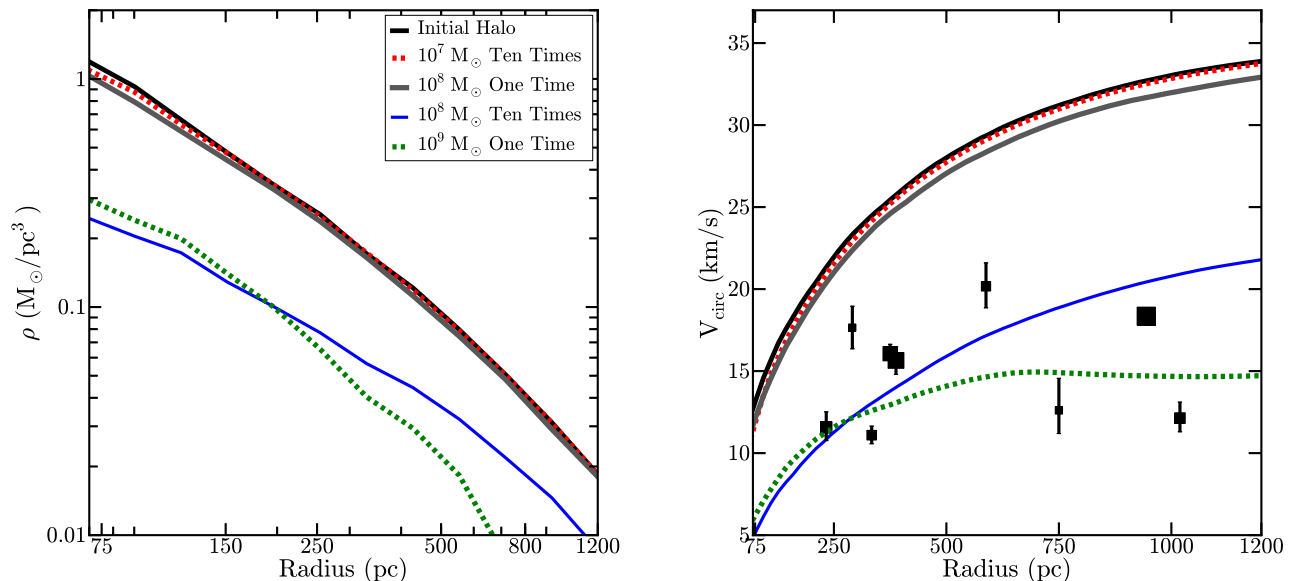


Figure 4. The density (left) and circular velocity (right) profiles of the halo after ten blowouts of $10^7 M_\odot$ and one blowout of $10^8 M_\odot$ (upper lines; as illustrated in Figure 3), and after ten blowouts of $10^8 M_\odot$ and one blowout of $10^9 M_\odot$ (lower lines), all with $r_{1/2} = 500$ pc (the qualitative results are similar for $r_{1/2} = 100$ pc). Removing $10^7 M_\odot$ ($10^8 M_\odot$) ten times is less effective at removing dark matter from the inner region of the halo than removing $10^8 M_\odot$ ($10^9 M_\odot$) once. Furthermore, note that $\sim 10^9 M_\odot$ must be blown out of the halo to bring the circular velocity into agreement with the data.

Another way to characterize the problem inherent in lowering the densities in the faintest dwarfs is to consider the energy required to bring densities into accordance with observations (Peñarrubia et al. 2012). The right hand panel of Figure 5 presents the mass remaining within 500 pc as a function of the cumulative energy injected into the dark matter after a series of $10^7 M_\odot$ (squares) and $10^8 M_\odot$ (triangles) blowouts for two values of $r_{1/2}$. Green symbols correspond to $r_{1/2} = 100$ pc blowouts and the black symbols correspond to $r_{1/2} = 500$ pc blowouts. The smaller $r_{1/2}$ runs produce marginally bigger effects for the same energy. However, the three dwarfs shown by bands in Figure 5 have $r_{1/2} \simeq 600$ pc, 900 pc, and 1000 pc, respectively. Thus we regard our 100 pc blowout models as quite conservative limits.

We calculate the energy injected into the dark matter by measuring the energy difference in the dark matter before and after each blowout. We ignore the energy “lost” when the dark matter re-contracts in response to central potential regrowth. This is because we are interested in the energy imparted to the dark matter by explosive feedback, which has nothing to do with how the gas falls back in to regrow the central galaxy (ignoring this component amounts to changes in the presented values at the factor of ~ 2 level). For our fiducial runs with $r_{1/2} = 500$ pc, we see that more than 4×10^{55} ergs of energy must be delivered to the dark matter before the inner mass becomes consistent with Ursa Minor. Assuming an energy per explosion of $E_{SN} = 10^{51}$ erg, this corresponds to more than 40,000 supernovae worth of energy injected directly into the dark matter with 100% coupling. Given that we expect approximately one SNII explosion per $100 M_\star$ formed for a typical IMF (Kroupa 2002), this exceeds the total available energy budget for all of the

type II supernova that have occurred in Ursa Minor. Indeed, it exceeds the associated supernovae budget for six of the nine galaxies of concern in Figure 1, all of which, according to extrapolated abundance matching, should be sitting in massive halos. The three most luminous dSphs may be in the range of viability, but we must assume that the energy couples directly to the dark matter, ignoring the energy required to expel the gas from the halo and radiative losses. The real energetic requirements may be more than a factor of 10 larger (Creasey et al. 2012). We also note that a single, large blowout injects more energy into the dark matter than is imparted by ten successive, smaller blowouts of the same total mass.

As discussed above, Fornax (with $r_{1/2} \simeq 1$ kpc and $L_V \simeq 1.7 \times 10^7 L_\odot$) appears to be the best candidate for having its density lowered significantly by feedback effects. We expect Fornax to have had $\sim 3 \times 10^5$ supernovae explosions over its history. According to Figure 5, a $\sim 20\%$ coupling of E_{SN} to the dark matter could in principle have lowered the central density of a 35 km/s halo enough to match the observed density of Fornax. Interestingly, however, if we run multiple blowouts at $\sim 10^9 M_\odot$, we find that our host halo becomes unbound all together. This suggests that even in cases where the required blowout is plausible energetically, there is something of a fine-tuning problem: if feedback is really as effective as required, then many of these halos should be destroyed all together. If this level of coupling is generic, one might expect slightly more star-rich galaxies to not exist at all.

One of the main results presented above is that repeated, cyclic blowouts do not help in lowering the central densities of galaxies compared to single bursts. However,

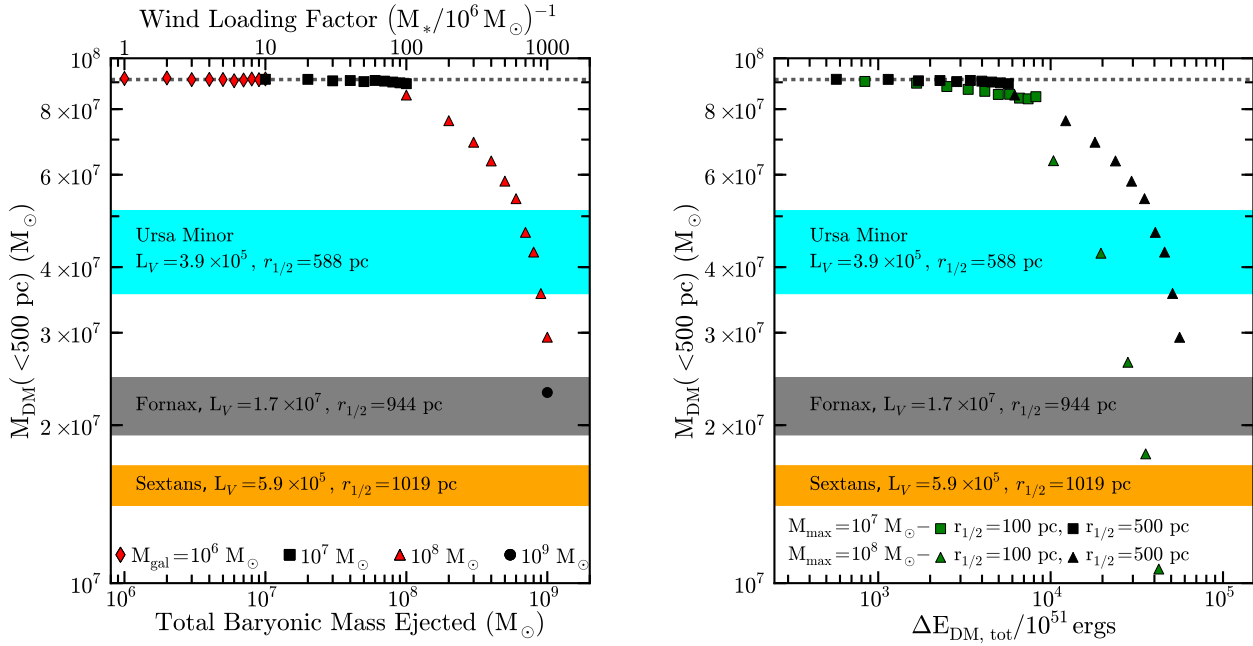


Figure 5. *Left:* The mass remaining within 500 pc after repeated blowouts of a galaxy with $M_{\text{max}} = 10^6, 10^7, 10^8$, and $10^9 M_{\odot}$, all with $r_{1/2} = 500$ pc, as a function of mass blown out. *Right:* The mass remaining after blowouts of $10^7 M_{\odot}$ and $10^8 M_{\odot}$ with either $r_{1/2} = 100$ pc (in green) or 500 pc (in black) as a function of the cumulative change in the dark matter energy. The dotted line indicates the original mass within 500 pc, and the colored bands indicate the dark matter within 500 pc for Ursa Minor, Fornax, and Sextans. As the stellar component of Fornax contributes non-negligibly to the mass near its center, we have subtracted $7 \times 10^6 M_{\odot}$ from the dynamical mass in order to account for the stellar mass within 500 pc for this galaxy (Jardel & Gebhardt 2012). More than several times $10^8 M_{\odot}$ must be ejected to bring the mass into agreement with Ursa Minor, and the requisite energy also exceeds the total supernovae budget for six of the nine classical dSphs. Furthermore, we note that ΔE_{DM} is a lower limit on the energy that must be injected, as it does not account for energy escaping via radiation or the energy required to eject the baryons.

we find that for a fixed amount of mass expelled, cyclic blowouts preferentially remove dark matter mass from the centers of halos, making them more effective at shallowing cusps. We find that the effect is most dramatic for the smallest $r_{1/2}$ runs. Figure 6 compares the density profile after ten blowouts of $M_{\text{max}} = 10^7 M_{\odot}$ to one blowout with $M_{\text{max}} = 10^8 M_{\odot}$, both with $r_{1/2} = 100$ pc. We see that several small blowouts begins to flatten the density profile at the center of the halo, whereas one large blowout displaces mass more evenly at all radii. Though a thorough investigation of this is outside the scope of this work, there does appear to be evidence that the scheme proposed by Pontzen & Governato (2012) can lead to more core-like dark matter profiles, but it appears unlikely that it can remove enough mass to resolve the TBTF problem. Moreover, we are never able to produce true constant-density cores. Rather we find mild cusps, $\rho \propto r^{-\alpha}$, slightly steeper than $\alpha \sim 0.5$.

4 CONCLUSIONS

In this paper we have used a series of idealized numerical experiments to investigate whether blowout feedback can plausibly resolve the Too Big to Fail (TBTF) problem for subhalos seen in Λ CDM simulations (Boylan-Kolchin et al. 2011, 2012). We relied on a tunable central potential to mimic the effects of cyclic baryonic feedback events within a $V_{\text{max}} = 35$ km/s halo – the mass scale of concern for the TBTF problem. Our main conclusions are as follows.

- In order to bring massive subhalo densities in line with those observed for Milky Way dSphs, a total of $\sim 10^9 M_{\odot}$ of material must be ejected. This is close to (and marginally exceeding) the baryonic allotment for the halos of concern and requires wind loading factors in excess of ~ 500 for the majority of Milky Way satellites.
- Our fiducial feedback models that match the observed densities of Milky Way dwarfs require the deposition of $>40,000$ supernovae worth of energy directly into the dark matter with 100% efficiency. For typical initial mass functions, this exceeds the expected number of Type II supernova explosions for six of the nine brightest dSph satellites. The most plausible exception is Fornax, with a density that may be explained with a $\sim 20\%$ coupling of its full allotment of SN energy directly to the dark matter. If this were the case it might pose a fine-tuning problem for slightly more luminous galaxies, as they might be expected to completely unbind their host halos.
- Repeated blowouts are less effective at lowering the central densities of dark matter halos than a single blowout of the same cumulative mass. They also impart less energy to the dark matter for the same total gas mass ejected. The main advantage of cyclic blowouts, from a density reduction perspective, appears to be in producing a shallower central cusp because dark matter is preferentially removed at small radii, though the overall density is higher at all radii (see Figure 6). However, we are unable to produce a true constant-

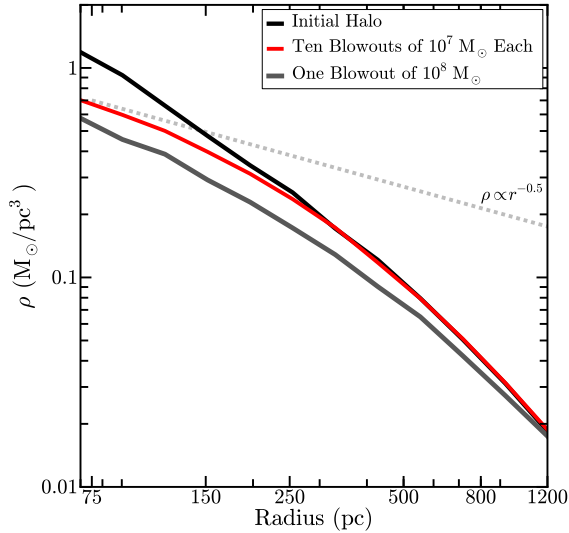


Figure 6. The density profile of the halo after ten blowouts of $10^7 M_\odot$ and one blowout of $10^8 M_\odot$ with $r_{1/2} = 100$ pc. As with blowouts with $r_{1/2} = 500$ pc, repeated blowouts are less effective than a single, more massive, blowout at displacing dark matter. However, repeated small blowouts from the very center of the halo do begin to flatten the inner density profile, whereas a more massive potential removes mass even at $10r_{1/2}$.

density core from cyclic blowouts, even in the most extreme cases.

This work has focused on the effects of internal feedback on the density structure of dark matter halos that are similar to those that will become massive subhalos in Milky Way-mass halos at redshift zero. We have not considered the effects of subsequent tidal evolution that will be relevant for some Milky Way subhalos (Brooks & Zolotov 2012; Zolotov et al. 2012; Arraki et al. 2012). We note, however, that several Milky Way dSphs do not seem to have had close pericentric passages with the Galaxy (Lux et al. 2010; Sohn et al. 2012), and it is far from clear that tidal effects will be able to reduce the density of “massive failures” enough to bring them into agreement with observations. Indeed, Arraki et al. (2012) have shown that tidal evolution alone is insufficient to bring the simulated subhalo population into agreement with observations of the MW dSphs. In light of these uncertainties, the results presented here point to isolated, low-mass galaxies as particularly important objects for testing the supernova feedback model for dark matter density reduction. Future optical and radio surveys will be capable of detecting objects with stellar masses similar to the MW dSphs outside of the Local Group; comparing their density structure to predictions from simulations will be strongly constraining for models of supernova feedback.

Acknowledgments

This work was funded in part by NSF grants AST-1009999, AST-1009973, and NASA grant NNX09AD09G. M.B.-K. acknowledges support from the Southern California Center for

Galaxy Evolution, a multi-campus research program funded by the University of California Office of Research. J.S.B. was partially supported by the Miller Institute for Basic Research in Science during a Visiting Miller Professorship in the Department of Astronomy at the University of California Berkeley. The authors thank Manoj Kaplinghat for insightful discussions.

References

- Arraki, K. S., Klypin, A., More, S., & Trujillo-Gomez, S. 2012, ArXiv e-prints
- Behroozi, P. S., Wechsler, R. H., & Conroy, C. 2012, ArXiv e-prints
- Boylan-Kolchin, M., Bullock, J. S., & Kaplinghat, M. 2011, MNRAS, 415, L40
- . 2012, MNRAS, 422, 1203
- Brooks, A. M., & Zolotov, A. 2012, ArXiv e-prints
- Bullock, J. S., & Johnston, K. V. 2005, ApJ, 635, 931
- Creasey, P., Theuns, T., & Bower, R. G. 2012, ArXiv e-prints
- de Blok, W. J. G. 2010, Advances in Astronomy, 2010
- Diemand, J., Kuhlen, M., Madau, P., et al. 2008, Nature, 454, 735
- Flores, R. A., & Primack, J. R. 1994, ApJ, 427, L1
- Governato, F., Zolotov, A., Pontzen, A., et al. 2012, MNRAS, 422, 1231
- Guedes, J., Callegari, S., Madau, P., & Mayer, L. 2011, ApJ, 742, 76
- Guo, Q., White, S., Li, C., & Boylan-Kolchin, M. 2010, MNRAS, 404, 1111
- Hernquist, L. 1990, ApJ, 356, 359
- Hinshaw, G., Larson, D., Komatsu, E., et al. 2012, ArXiv e-prints
- Ho, S., Cuesta, A., Seo, H.-J., et al. 2012, ApJ, 761, 14
- Jardel, J. R., & Gebhardt, K. 2012, ApJ, 746, 89
- Kazantzidis, S., Mayer, L., Mastrogiuseppe, C., et al. 2004, ApJ, 608, 663
- Kroupa, P. 2002, Science, 295, 82
- Kuzio de Naray, R., & Kaufmann, T. 2011, MNRAS, 414, 3617
- Kuzio de Naray, R., McGaugh, S. S., & de Blok, W. J. G. 2008, ApJ, 676, 920
- Lux, H., Read, J. I., & Lake, G. 2010, MNRAS, 406, 2312
- Mashchenko, S., Couchman, H. M. P., & Wadsley, J. 2006, Nature, 442, 539
- Moore, B. 1994, Nature, 370, 629
- Navarro, J. F., Eke, V. R., & Frenk, C. S. 1996, MNRAS, 283, L72
- Ogiya, G., & Mori, M. 2012, ArXiv e-prints
- Peñarrubia, J., Pontzen, A., Walker, M. G., & Koposov, S. E. 2012, ApJ, 759, L42
- Pontzen, A., & Governato, F. 2012, MNRAS, 421, 3464
- Rocha, M., Peter, A. H. G., Bullock, J. S., et al. 2012, ArXiv e-prints
- Sohn, S. T., Besla, G., van der Marel, R. P., et al. 2012, ArXiv e-prints
- Springel, V. 2005, MNRAS, 364, 1105
- Springel, V., Wang, J., Vogelsberger, M., et al. 2008, MNRAS, 391, 1685

- Strigari, L. E., Bullock, J. S., Kaplinghat, M., et al. 2008, *Nature*, 454, 1096
- Teyssier, R., Pontzen, A., Dubois, Y., & Read, J. 2012, ArXiv e-prints
- Trachternach, C., de Blok, W. J. G., Walter, F., Brinks, E., & Kennicutt, Jr., R. C. 2008, *AJ*, 136, 2720
- Vogelsberger, M., Zavala, J., & Loeb, A. 2012, ArXiv e-prints
- Walker, M. G. 2012, ArXiv e-prints
- Wolf, J., Martinez, G. D., Bullock, J. S., et al. 2010, *MNRAS*, 406, 1220
- Zemp, M., Moore, B., Stadel, J., Carollo, C. M., & Madau, P. 2008, *MNRAS*, 386, 1543
- Zolotov, A., Brooks, A. M., Willman, B., et al. 2012, ArXiv e-prints